


# The Design of H-infinity Controllers for an Experimental Non-collocated Flexible Structure Problem

**Journal Article****Author(s):**

Smith, Roy ; Chu, Cheng-Chih; Fanson, James L.

**Publication date:**

1994-06

**Permanent link:**

<https://doi.org/10.3929/ethz-b-000125920>

**Rights / license:**

In Copyright - Non-Commercial Use Permitted

**Originally published in:**

IEEE Transactions on Control Systems Technology 2(2), <https://doi.org/10.1109/87.294333>

# The Design of $H_\infty$ Controllers for an Experimental Non-collocated Flexible Structure Problem

Roy S. Smith, Cheng-Chih Chu, and James L. Fanson

**Abstract**—This paper describes recent results in applying robust control techniques to achieve vibration suppression of an active precision truss structure. The active structure incorporates piezoelectric members which serve as both structural and actuation elements. The problem considered is multiple-input, multiple-output with non-collocated actuators and sensors. Several characterizations of uncertainty are studied and the resulting controllers are compared experimentally. One characterization uses a novel approach involving eigenvalue perturbation descriptions.

**Index Terms**—Robust control, flexible structures.

## I. INTRODUCTION

The Control Structure Interaction (CSI) program at the Jet Propulsion Laboratory is investigating the technology required to achieve submicron level dimensional stability on large complex optical class spacecraft. The focus mission for this work is an orbiting interferometer telescope [1]. A series of evolutionary testbed structures are being constructed for the purpose of developing and demonstrating the technology required for such a mission. The JPL CSI Phase 0 testbed structure, described in Section II, is one in a series of experimental facilities used for the development of active structure hardware and feedback control methodologies [2]. This structure is the experimental testbed for the robust control designs described here.

Achieving submicron stability of the optical system involves a layering of several technologies including active vibration isolation, structural vibration suppression, and active optical control. The work considered here applies to the active vibration suppression problem. A mixture of technologies can be applied to the vibration suppression problem itself; passive damping, active damping and active structural stabilization. Refer to [3] for earlier work on the application of all of these technologies to the Phase 0 experiment. This paper concentrates only on the active structural stabilization work and includes more recent approaches and experimental results.

The wider issue of vibration suppression, particularly in flexible space systems, is an active area of research. Many approaches have been applied at a number of institutions, and no attempt is made here to give a complete summary. A similar approach is described by Balas and Doyle [4].

The robust control approach requires a nominal model and a description of the uncertainty. This uncertainty description often takes the form of norm bounded perturbations occurring at various places within the nominal model. The resulting control design achieves specified performance and stability characteristics for all system models described by the set of bounded perturbations. This is a powerful approach as one not only designs a controller for a specified model, but also for models “close” to that model. In other words the design is robust with respect to perturbations in the system model. The underlying hope is that the perturbations in the model describe the various uncertain behaviors of the physical system.

A more complicated identification problem arises as a result of the robust control approach. One must now specify perturbation bounds in addition to the nominal system model. Model structural choices — the number of perturbations and how each perturbation enters the model — must also be made. Currently there is little theory addressing these issues. Ad-hoc approaches must be used and one hopes that experience on a particular problem is representative for similar problems. The issue of uncertainty modeling is specifically addressed in this paper. Three choices of perturbation structure have been studied experimentally, and the results are presented here.

The experimental problem is described in detail in Section II. The flexible structure context of this work has been described elsewhere [1,2,5,6] and only the salient issues will be mentioned here. Obtaining a nominal model from experimental data is itself a difficult problem. This is described in detail in [7] and summarized in [3].

The  $H_\infty/\mu$  synthesis methodology was used for all of the designs. Refer to [8] for algorithmic and general application details of this approach. A brief overview of the approach is given in Section III, where the flexible structure problem is used to illustrate the theory.

The perturbation structures studied are outlined in Section IV. Uncertainty in flexible structures is often characterized as uncertainty in the modal frequencies and damping ratios. When the standard  $H_\infty$  perturbation models are applied to this problem the resulting model can be dominated by the perturbation which may lead to a conservative design. An alternative perturbation modeling approach, based on perturbations to a state-space representation, can avoid this problem. This approach is also studied experimentally in this paper.

Particular choices of perturbation bounds and perturbation structure result in different controllers. Three such controllers,  $K_1$ ,  $K_2$  and  $K_3$ , are described in Section IV. The performance of all three designs is evaluated on the experiment in Section V.

R.S. Smith is with the Dept. of Electrical & Computer Engineering, University of California, Santa Barbara, CA 93106

C.-C. Chu is with the Guidance and Control Section, Jet Propulsion Laboratory, California Institute of Technology, Pasadena, CA 91109

J.L. Fanson is with the Applied Mechanics Technologies Section, Jet Propulsion Laboratory, California Institute of Technology, Pasadena, CA 91109

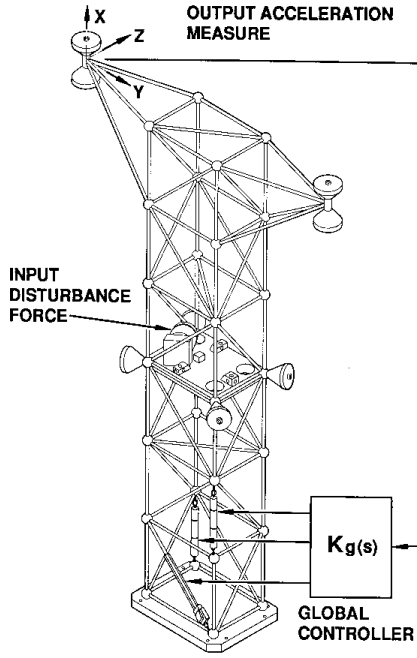


Fig. 1. Precision truss structure. The control design problem inputs and outputs are also illustrated

The paper concludes (Section VI) with a discussion of the various perturbation model choices and speculates on the applicability of robust control to the design of spacecraft vibration damping systems.

## II. EXPERIMENTAL DESCRIPTION

The Phase 0 Precision Truss is a six bay structure, approximately 2 meters tall, with two outriggers at the top. The base is cantilevered off of a massive steel block. The total mass of the structure is approximately 27 kg and was designed to have very low damping. The modes of the structure (up to 60 Hz) are divided into two groups, the first group is near 10 Hz, and the higher group starts at approximately 30 Hz. The 30–40 Hz modes involve significant local bending of the truss members and are therefore only marginally controllable from the location of the active members. The structure is extremely lightly damped with the damping ratios of the first eleven modes ranging from 0.0008 to 0.015.

Accelerometers, mounted on an outrigger, measure the X, Y and Z direction accelerations. Three active members (denoted AM), located in the lower two bays, are used for control. A disturbance is injected, via a shaker, at the middle bay. The control objective is the minimization of the experimentally estimated transfer function from the midbay disturbance to the three accelerometers, for a bandwidth including at least the first three modes (up to  $\approx 15$  Hz). Figure 1 illustrates the configuration of the structure and the control problem to be studied.

Piezoelectric actuators, built into the active members, provide the force actuation. These are capable of delivering a clamped force of 1810 N, for the vertical members, and 430 N for the diagonal member, at input voltages of 1000 Volts

and 150 Volts respectively. Commercial amplifiers provide the necessary high bandwidth gain and bias the actuators to their midpoints. Anderson *et al.* [9] detail the construction of these actuators. Commercial micro-g accelerometers provide the X, Y and Z direction acceleration measurements. The accelerometer outputs are amplified and filtered (2nd order Bessel filter with cut-off frequency of 1 kHz) prior to measurement by the data acquisition and control systems. Fanson *et al.* [6] provide greater detail on the structure and control related instrumentation.

The Hugh 9000, a VME bus based, real-time, control system was developed at JPL for the CSI program [10,11]. A Heurikon V3E processor card, based on a 25 MHz 68030 microprocessor, and a CSPI Quickcard array processor are used for the controller computations. The A/D and D/A conversion (16 bit resolution) is performed by Data Translation boards. For the controllers tested here the sampling rate was 1 kHz and the computational delay was 1 sample period (1 msec.). The number of controller states varied between 31 and 40.

## III. AN OVERVIEW OF $H_\infty/\mu$ ROBUST CONTROL

### A. Robust Control Models

The modeling framework to be applied here is presented in more detail by Packard [12]. Systems are modeled as nominal linear time-invariant systems with stable, linear-time invariant, perturbations. The perturbations, denoted by  $\Delta(s)$ , or more simply,  $\Delta$ , are assumed to be bounded by  $\|\Delta\|_\infty \leq 1$ , with

$$\|\Delta\|_\infty := \sup_{s=j\omega} \bar{\sigma}(\Delta(s)),$$

where  $\bar{\sigma}$  denotes the maximum singular value. A simple model might consist of the set described by  $P(s) + W(s)\Delta$ , where  $P(s)$  is the nominal model,  $W(s)$  is a frequency dependent weight, and  $\Delta$  is the unknown bounded perturbation. This is an additive perturbation description — the general situation can be described by a linear fractional transformation (LFT), on a block matrix,  $M$ , with inputs  $w$  and outputs,  $e$ , by,

$$\begin{aligned} e &= [M_{22} + M_{21}\Delta(I - M_{11}\Delta)^{-1}M_{12}] w \\ &=: F_u(M, \Delta) w. \end{aligned} \quad (1)$$

By appropriate choice of  $M_{11}$ , etc., the LFT form can be used to describe any interconnection of a nominal system with a perturbation. Furthermore,  $\Delta$  can be defined as having a specified block diagonal structure,

$$\Delta = \text{diag}(\Delta_1, \dots, \Delta_m), \quad (2)$$

and then (1) can describe perturbations occurring at different places in a complex interconnected system. Figure 2a illustrates the generic LFT of (1) in block diagram form. This representation is powerful because interconnections of LFTs are simply larger LFTs.

### B. Analysis of Stability and Performance

The robustness analysis discussed here was introduced by Doyle *et al.* [13,14]. For the following analysis procedure each component of  $M$  is assumed to be stable. The following problem is known as the robust stability problem:

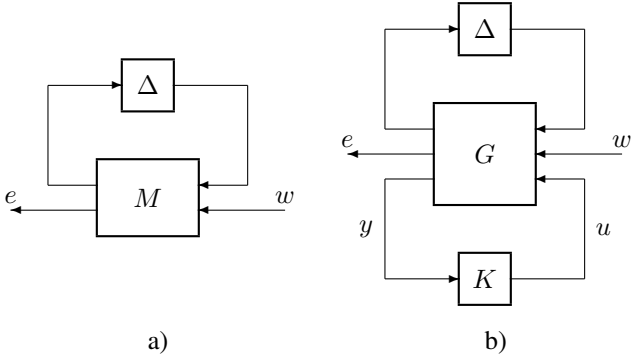


Fig. 2. a) Generic LFT system model, b) Interconnection for the design problem

Is  $F_u(M, \Delta)$  stable for all perturbations,  $\Delta$ ,  $\|\Delta\|_\infty \leq 1$ ? In the case where  $\Delta$  has no block diagonal structure, the answer is as follows.  $F_u(M, \Delta)$  is robustly stable if and only if  $\|M_{11}(s)\|_\infty < 1$ . In the case where we are dealing with several perturbations (e.g.  $m$  perturbations modeled by  $\Delta$  as in (3), the structured singular value, denoted by  $\mu$ , provides the answer. The interconnection,  $F_u(M, \Delta)$  is robustly stable if and only if  $\|\mu(M_{11}(s))\|_\infty < 1$ . Note that  $\mu$  is a function of the prescribed block diagonal structure given in (3). For the typical engineering problems that arise here  $\mu$  can usually be quickly calculated to within 5%.

A similar result holds for robust performance if performance is appropriately defined. The following framework will be used throughout for the study of performance. In Fig. 2a the inputs,  $w$ , are assumed to be unknown but bounded. They would typically represent noise, disturbances or tracking commands. The outputs,  $e$ , represent signals which are required to be small in a particular norm. These might typically be error signals and actuator outputs. In the problem considered here,  $w$  will consist of the unknown midbay acceleration input and noise on the accelerometer measurements. The X, Y and Z accelerations, and the controller outputs are modeled as the signal  $e$ .

Any frequency dependent weighting on the signals is factored into  $M$  so that specified nominal performance is equivalent to  $\|M_{22}(s)\|_\infty < 1$  and robust performance is  $\|F_u(M, \Delta)\|_\infty < 1$  for all  $\Delta$ , of the appropriate structure, satisfying  $\|\Delta\|_\infty \leq 1$ . The system satisfies the robust performance specification if and only if  $\|\mu(M)\|_\infty < 1$ . If it satisfies robust performance it necessarily satisfies robust stability.

The above result is typically applied when  $M$  represents a closed loop system. The associated design problem is illustrated in Fig. 2b. Given a weighted perturbation model,  $G$ , design  $K$  to stabilize  $G$  and satisfy the robust performance test. The signals  $y$  are the controller measurements and  $u$  are the actuator signals. In the nominal, unperturbed, case ( $\Delta = 0$ ) this problem is solved by the  $H_\infty$  design procedure [15]. In the more general  $\Delta$  perturbation case an iterative procedure (known as  $D$ - $K$  iteration) gives controllers that approximate the solution [8]. This procedure is discussed in greater detail in Section III.C.

The choice of the  $\infty$ -norm as a measure of performance

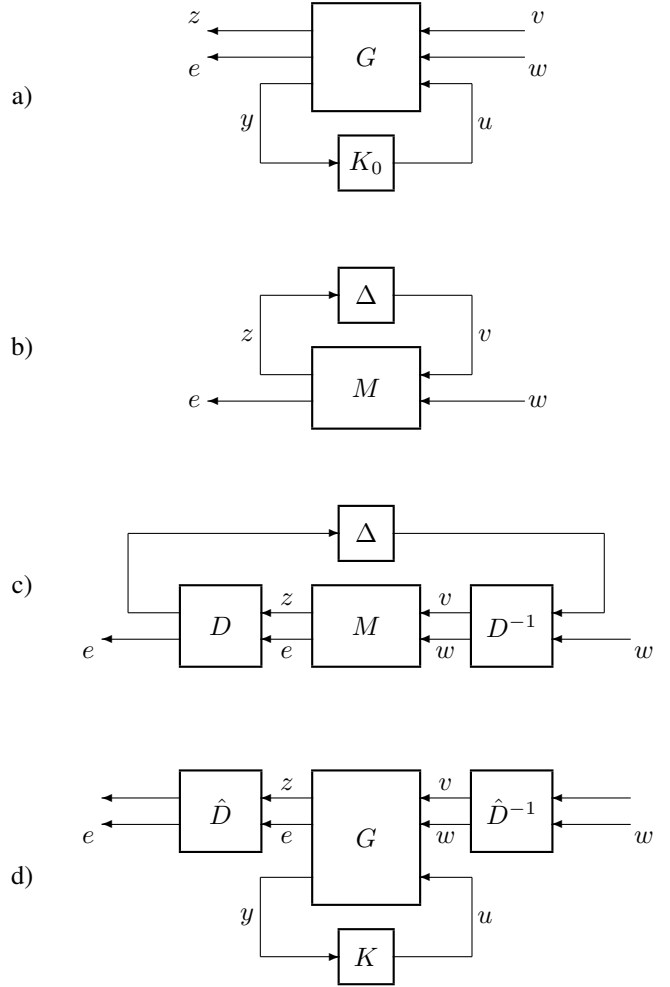


Fig. 3.  $D$ - $K$  iteration procedure: a) Design  $H_\infty$  controller,  $K_0$ . b) Closed loop perturbed system for  $\mu$  analysis. c) Upper bound  $D$  scale approximation to  $\mu$  analysis. d) Scaling of  $H_\infty$  design problem by  $\hat{D}$  where  $\hat{D} \approx D$  from upper bound  $\mu$  calculation.

leads to the computationally tractable robust synthesis problem above. This may not be an ideal choice from an engineering point of view. If  $w$  is bounded in energy (or power) then this method minimizes the energy (or power) of  $e$ . Bounded energy signals may be poor representations of noise or command references. Similarly one may be interested in other choices of output error specification. This paper will illustrate, by example, that on physically motivated problems, the  $H_\infty/\mu$  synthesis controllers can also perform well by other measures. In this specific example,  $w$  will include the shaker input disturbance and  $e$  will include the weighted accelerations. Minimizing the  $\infty$ -norm will reduce the peak of this transfer function. In our application the damping ratios of the lower frequency modes are significantly increased.

In order to apply this approach, one must obtain a nominal model and perturbation description for the system. Several choices of perturbation descriptions are studied in Section IV.

### C. Controller Synthesis with $D$ - $K$ Iteration

The  $D$ - $K$  iteration procedure is illustrated schematically in Fig. 3. An  $H_\infty$  design is performed (Fig. 3a) to get an initial controller,  $K_0(s)$ . This minimizes  $\|M(s)\|_\infty$ , where  $M(s)$  is the closed loop system with controller  $K_0(s)$ . This is an upper bound on the desired objective,  $\|\mu(M(s))\|_\infty$  (Fig. 3b).

At each frequency, a scaling matrix,  $D$ , can be found such that  $\bar{\sigma}(DMD^{-1})$  is a close upper bound to  $\mu(M)$  (Fig. 3c). The  $D$  scale is block diagonal and the block corresponding to the  $e$  and  $w$  signals can be chosen to be the identity. The part of  $D$  corresponding to the  $z$  signal commutes with  $\Delta$  and cancels out the part of  $D^{-1}$  corresponding to the  $v$  signal. Therefore  $\mu(DMD^{-1}) = \mu(M)$  and the robust performance analysis is unaffected.

However the  $H_\infty$  design problem is strongly affected by scaling. The synthesis approach involves applying the  $D$  scaling to the original  $H_\infty$  design problem. The  $D$  scale is a complex valued matrix at each frequency and an approximate realization (denoted by  $\hat{D}$  in Fig. 3d) must be obtained before it can be applied to the state-space  $H_\infty$  design (Fig. 3d). The resulting controller,  $K$ , gives a new closed loop system,  $M$ , with  $\mu(M)$  smaller than that given by the controller  $K_0$ . The procedure can be iterated upon (Figs. 3b through 3d):  $\mu$  analysis of the new closed loop system gives a different  $D$  scale and this can be applied to the  $H_\infty$  design problem.

Several aspects of this procedure are worth noting. For the  $\mu$  analysis and  $D$  scale calculation, a frequency grid must be chosen. The range and resolution of this grid is a matter of engineering judgement. The  $\mu$  analysis can require a fine grid in the vicinity of the lightly damped modes. The order of the initial controller,  $K_0$ , is the same as the interconnection structure,  $G$ . The order of  $K$  is equal to the sum of the orders of  $G$ ,  $\hat{D}$  and  $\hat{D}^{-1}$ . This leads to a trade-off between the accuracy of the fit between  $D$  and  $\hat{D}$  and the order of the resulting controller  $K$ .

The robust performance difference between the  $H_\infty$  controller,  $K_0$ , and  $K$ , can be dramatic even after a single  $D$ - $K$  iteration. The  $H_\infty$  problem is sensitive to the relative scalings between  $v$  and  $w$  (and  $z$  and  $e$ ). The  $D$  scale effectively provides the optimal choice of relative scalings for closed loop robust performance.

## IV. SYSTEM MODELS AND PERTURBATION STRUCTURES

A nominal model, denoted by  $P_{\text{nom}}$ , has been identified by a multivariable approach based on estimated transfer functions and an iterative least squares optimization. This is described in detail in [7] and summarized in [3].

Three perturbation models are studied here, giving designs  $K_1$ ,  $K_2$  and  $K_3$ . The choice of perturbation structure and associated weighting functions drives the controller design. The first two are based on relatively standard perturbation modeling approaches. The modeling approach use to obtain  $K_3$  will be discussed in greater detail later in this section. The full design problem is covered to provide the necessary background to the perturbation description discussion.

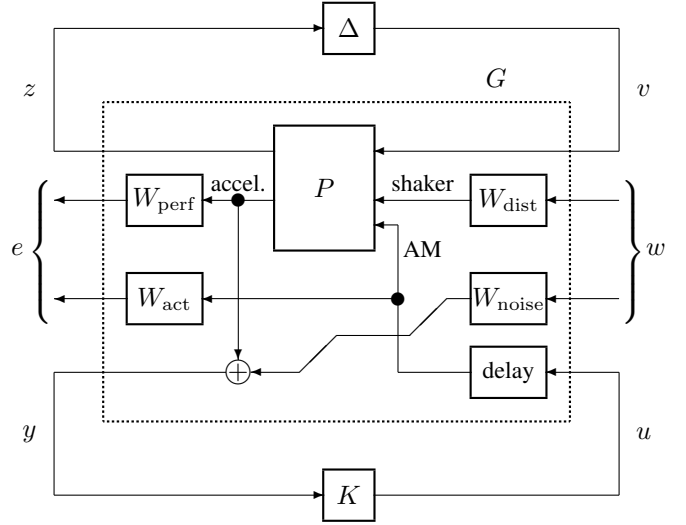


Fig. 4. Interconnection structure for the controller design

### A. Outline of the Design Problem

Figure 4 shows the weighted interconnection structure, denoted by  $G$ , used for the  $D$ - $K$  iteration. This corresponds to the block  $G$  in Figs. 2b and 3a. The three perturbation models ( $F_u(P, \Delta)$ ) were embedded in a generalized interconnection structure for each of the designs. The unknown inputs,  $w$ , are the shaker and weighted noise signals applied to each of the acceleration measurements. Weighted X, Y and Z accelerations, along with the weighted controller outputs, are considered as the error signals  $e$ . The controller calculation delay was modeled by a Padé approximation.

The weighting functions,  $W_{\text{perf}}$ ,  $W_{\text{act}}$ ,  $W_{\text{dist}}$  and  $W_{\text{noise}}$  act as the engineering design variables and were adjusted to investigate the achievable performance with each of the perturbation models. The most significant feature of the weighted problem is that  $W_{\text{dist}}$  is essentially bandlimited, having the effect of disregarding performance (vibration suppression) for frequencies above 15 Hz. High frequency actuator effort was also penalized. Refer to [3] for an example of representative weighting functions for an earlier version of this problem.

The  $H_\infty/\mu$  synthesis procedure produces controllers of order at least as high as that of the weighted interconnection used for the design. In this case this resulted in controllers of approximately 60th order. Although it is rapidly becoming less of a computational issue, most engineers are reluctant to implement what is essentially a “black box” controller of that order. One view is that such controllers give some estimate of the achievable performance and can be used as a benchmark with which to compare the results of more classical approaches. In this case the objective is to obtain some estimate of the achievable performance with robust control. Controller order reduction was performed via a combination of balanced truncation [16] and Hankel norm model reduction [17] as the real-time controller was limited to 40 states at 1000 Hz.

The solution of the  $H_\infty$  design equations can be numerically

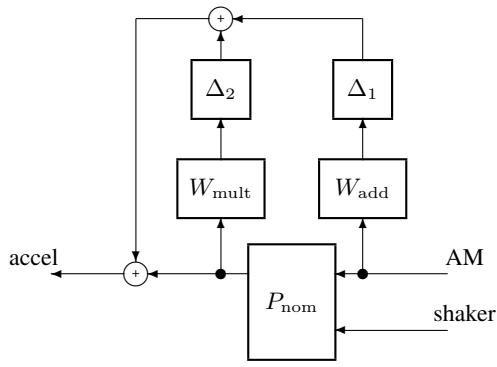


Fig. 5. Perturbation model for design  $K_1$

poorly conditioned for high order interconnection structures with lightly damped modes. The 60th order structure described above requires an ordered Schur decomposition of a  $120 \times 120$  Hamiltonian matrix. This was possible with the currently available software. Because of the dimension and number of perturbations, each state used in fitting a transfer function to a  $D$  scale results in an additional 12 states in the scaled interconnection structure. These additional states lead to a numerically unstable design problem, and to avoid this constant  $D$  scales were used. Even constant  $D$  scales resulted in a significant performance improvement over the standard  $H_\infty$  design.

### B. $K_1$ Perturbation Structure

The  $K_1$  perturbation structure is shown in Fig. 5. The perturbations are additive,  $\Delta_1$  weighted by  $W_{\text{add}}$ , and multiplicative,  $\Delta_2$  weighted by  $W_{\text{mult}}$ . Both of the weights are diagonal.

The dynamic perturbation weights for each control design are given in Fig. 6. For comparison purposes, the AM to X acceleration estimated transfer function is also shown. The diagonal components of all of these weights are individually scaled to account for differences in the relative sizes of the transfer functions.

The additive weight,  $W_{\text{add}}$ , increases sharply (3rd order roll-up) beyond the lower frequency (8–12 Hz) modes reflecting the fact that less is known about the system at higher frequencies. It will subsequently be seen that this weight is insufficient to describe the lack of information about the modes in the 30–40 Hz region. In the  $K_1$  design the weight  $W_{\text{mult}}$  is a small constant (0.05) intended to capture the possible mode-shape errors in the lower frequency modes.

### C. $K_2$ Perturbation Structure

The perturbation structure used for design,  $K_2$  is illustrated in Fig. 7. This structure reflects most possible combinations of additive and multiplicative perturbations. This is arguably excessively complicated — however it does allow one to investigate the effects of various perturbation locations. There can be a computational penalty in choosing too many perturbations. This is particularly true if a  $H_\infty$  design is performed, rather than a  $D$ - $K$  iteration ( $\mu$ -synthesis), as the  $\mu$ -synthesis

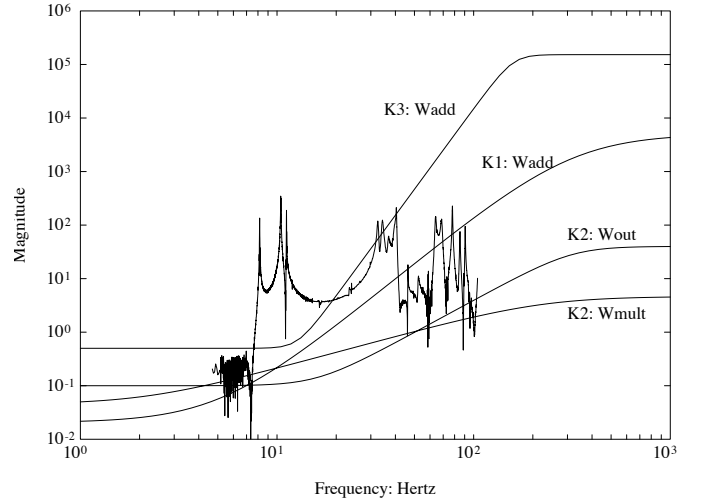


Fig. 6. Dynamic perturbation weights used in the system model for designs  $K_1$ ,  $K_2$  and  $K_3$ . Also illustrated is the AM to X estimated transfer function

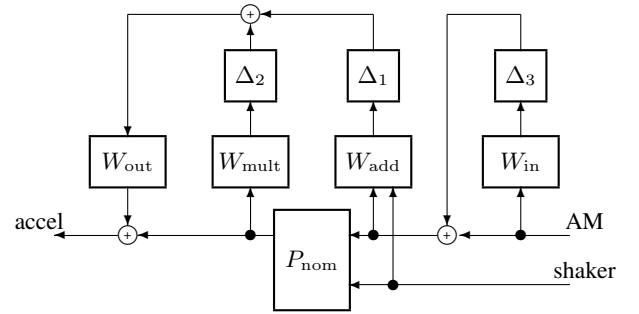


Fig. 7. Perturbation model for design  $K_2$

procedure can remove some of the conservatism introduced by an inappropriate choice of perturbation scalings.

In the  $K_2$  model case both  $W_{\text{mult}}$  and  $W_{\text{out}}$  increase with frequency (refer Fig. 6).  $W_{\text{add}}$  is a constant used as a relative scaling of the uncertainty with respect to the system inputs. Because of the different perturbation structures, a direct comparison of the weights is difficult. However, for the  $K_2$  case, the increase in uncertainty with frequency is reflected by the product of  $W_{\text{mult}}$  and  $W_{\text{out}}$  causing  $K_2$  to roll off significantly faster than  $K_1$ .

The  $K_2$  design also includes a small input multiplicative perturbation ( $W_{\text{in}} = 0.001$  for each active member input). This was found to make the controller model reduction easier. One possible explanation is that this reduces the tendency of the design methodology to generate a controller that inverts the plant from the input.

### D. $K_3$ Perturbation Structure

The approach taken here is to model the uncertainty in the lower frequency modes by an eigenvalue perturbation to the state-space representation. The higher frequency uncertainty is again described by an additive weight that increases with frequency. Figure 8 illustrates the perturbation structure. The additive perturbation,  $\Delta_1$ , again represents the high frequency

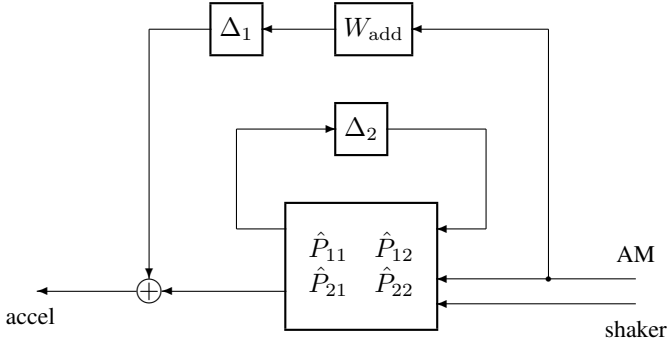


Fig. 8. Perturbation structure for design  $K_3$

uncertainty and the weighting function,  $W_{\text{add}}$ , is shown in Fig. 6.

This structure is significantly different in that the lower frequency uncertainty is represented by an LFT on the perturbation  $\Delta_2$ . The motivation for this approach is new and will now be discussed in more detail.

A particular LFT perturbation structure is chosen. Consider the nominal system to have a state-space representation,

$$P_{\text{nom}} = C(sI - A)^{-1}B + D.$$

The LFT is chosen as,

$$\begin{aligned} \hat{P}_{11} &= W_2(sI - A)^{-1}W_1 \\ \hat{P}_{12} &= W_2(sI - A)^{-1}B \\ \hat{P}_{21} &= C(sI - A)^{-1}W_1 \\ \hat{P}_{22} &= C(sI - A)^{-1}B + D, \end{aligned}$$

which yields the perturbed system,

$$F_u(\hat{P}, \Delta_2) = C(sI - A - W_1\Delta_2W_2)^{-1}B + D.$$

Note that this simply has the effect of replacing  $A$  by  $A + W_1\Delta_2W_2$ . A particular choice for  $A$ , motivated by the following result, is useful for modeling flexible structure perturbations.

Consider  $A$  to be real-valued and block diagonal, revealing the modal structure. If  $A$  has only  $n$  complex conjugate eigenvalue pairs,  $\lambda_{i\pm} = \sigma_i \pm j\beta_i$ ,  $i = 1, \dots, n$ , then the desired form of  $A$  is,

$$A = \begin{bmatrix} A_{11} & & \\ & \ddots & \\ & & A_{nn} \end{bmatrix}, \quad \text{where } A_{ii} = \begin{bmatrix} \sigma_i & \beta_i \\ -\beta_i & \sigma_i \end{bmatrix}.$$

A weighting matrix,  $W$ , is chosen to be diagonal;  $W \in \mathcal{R}^{2n \times 2n}$ ,

$$W = \begin{bmatrix} w_1 & & & \\ & w_1 & & \\ & & \ddots & \\ & & & w_n & \\ & & & & w_n \end{bmatrix}, \quad w_i > 0.$$

It is simple to show, via Geršgorin type arguments, that the eigenvalues of  $A + W\Delta_2$ , for all  $\bar{\sigma}(\Delta_2) \leq 1$ , lie within  $n$  pairs of disks, of radius  $w_i$ , centered at the eigenvalues of  $A$ ,

$\lambda_{i\pm}$ . For further details refer to [18,19]. The result trivially extends to systems with a combination of real and complex eigenvalues.

This approach is now used to model perturbations in the modal frequency and damping ratios of the lowest three modes. For this problem the weights  $W_1$  and  $W_2$  were chosen such that  $W = W_1W_2$  and only the lowest three modes have  $w_i > 0$ . This gave significantly lower input-output dimensions for  $\Delta_2$ .

An additional enhancement can also be made. In the above, the eigenvalues of  $A$ , are replaced by disks. By modifying selected  $A_{ii}$ , the centers of selected disks can be moved further into the left-half plane. This was done for the lowest three modes in this problem. Figure 9 illustrates the nominal eigenvalues (denoted by  $*$ ) and the shifted perturbation disk around each, for these modes. In this case the amount of uncertainty attributed to each mode was the same.

Uncertainty in a modal frequency and damping ratio corresponds to the eigenvalue lying within a rectangular region in the complex plane. In this case the shifted disks were chosen such that they would cover the rectangular regions corresponding to a 1% error in damping ratio and a 0.1% error in modal frequency. The centers of the disks correspond to new nominal eigenvalues and were chosen to be more heavily damped than the original nominal model. Note that this approach introduces additional plants into the perturbation model set which are unlikely to occur in practice. However these plants are more heavily damped and it is therefore hoped that they impose no additional difficulties on the control design problem.

Several practical benefits arise from this formulation. The nominal system is now more heavily damped leading to less numerical sensitivity in the control design algorithms. The associated perturbation ( $\Delta_2$  in this case) is weighted only by a constant which reduces the number of states in the design interconnection structure and therefore reduces the number of states in the resulting controller.

## V. EXPERIMENTAL RESULTS

Figure 10 shows the experimental transfer functions from the acceleration measured at the shaker input to the Y and Z accelerometer outputs. The X and Y acceleration responses are qualitatively similar for each of the controllers. The Z acceleration response is the worst case for each controller. The performance of controllers  $K_1$  and  $K_3$  is similar, with  $K_1$  being slightly better than  $K_3$ , and significantly better than  $K_2$ , particularly in the first mode.

The above statements must be considered in light of additional experimental experience. Controller  $K_1$  was tested several times over a period of a year. The earlier results are shown here. In later experiments the controller exhibited strong limit cycle behavior around 32 Hz, and in the latest series of experiments the closed loop system was unstable. This suggests slight variations in the structure have occurred over the period of a year. Although the experimental set-up was nominally identical in each case, the structure is part of a larger experimental program and the active members had been

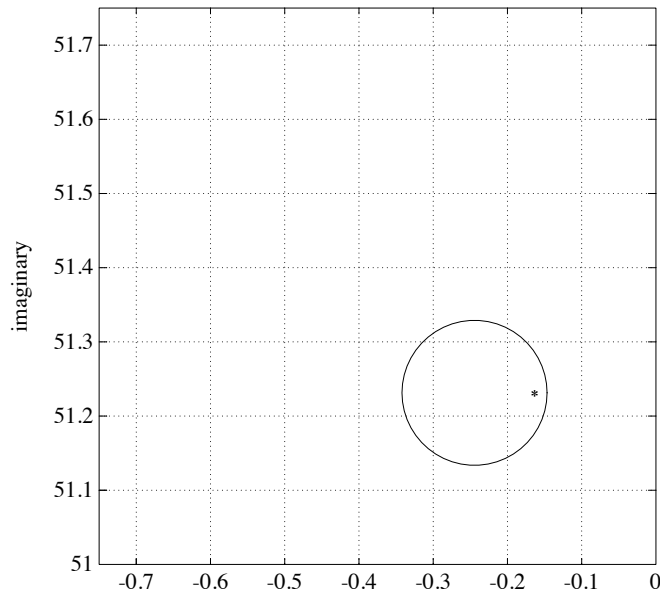
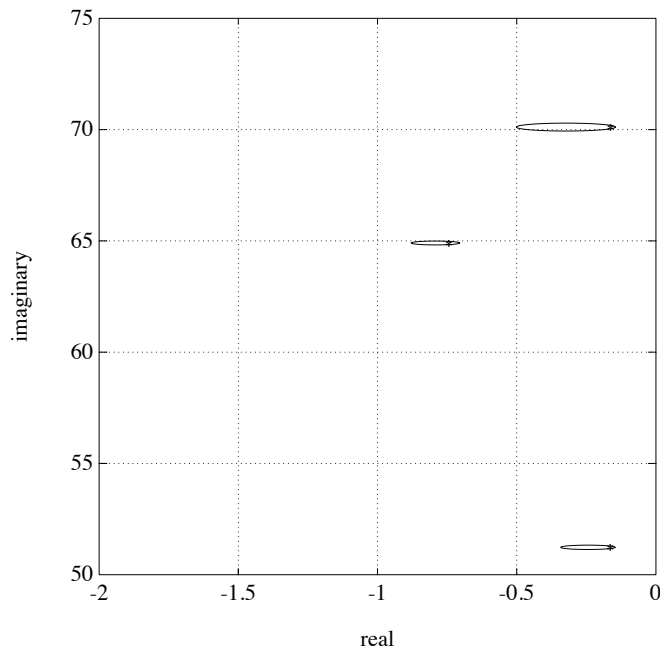


Fig. 9. Nominal eigenvalues, \*, and perturbation disks for lowest three modes. Lower figure shows only the lowest mode with the correct aspect ratio

removed and reinstalled in the structure several times. This is likely to have caused experiment to experiment differences.

Some indication of why  $K_1$  is so sensitive to such variation can be obtained by examining the singular values of the system loop gain. The maximum singular values of the loop gain are shown in Figure 11.

The maximum singular value of the loop gain is greater than one for several of the 30–40 Hz modes, indicating that these modes are not gain stabilized. The fact that the controller functioned at all indicates that it is possible to roll-off through these modes. However, the subsequent stability problems sug-

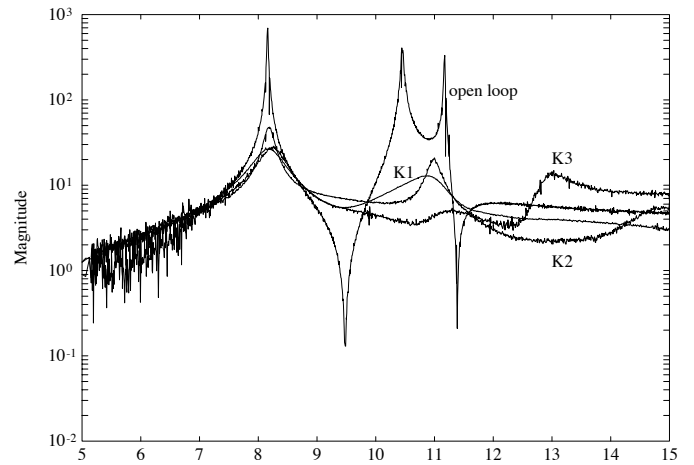
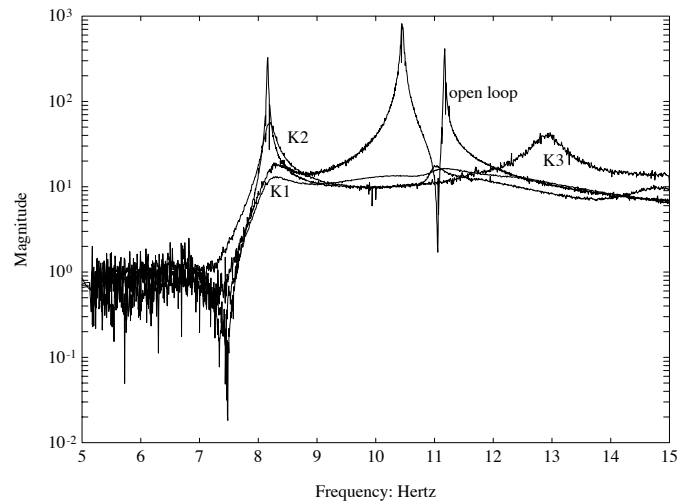


Fig. 10. Experimental estimated transfer functions for open and closed-loop systems. Upper plot: shaker acceleration to Y acceleration; lower plot: shaker acceleration to Z acceleration

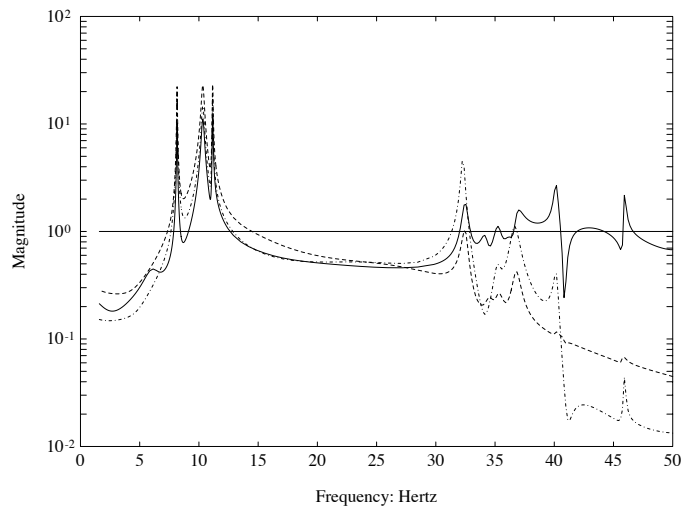


Fig. 11. Maximum singular value of the loop gains for  $K_1$  (solid),  $K_2$  (dashed) and  $K_3$  (dot-dash)



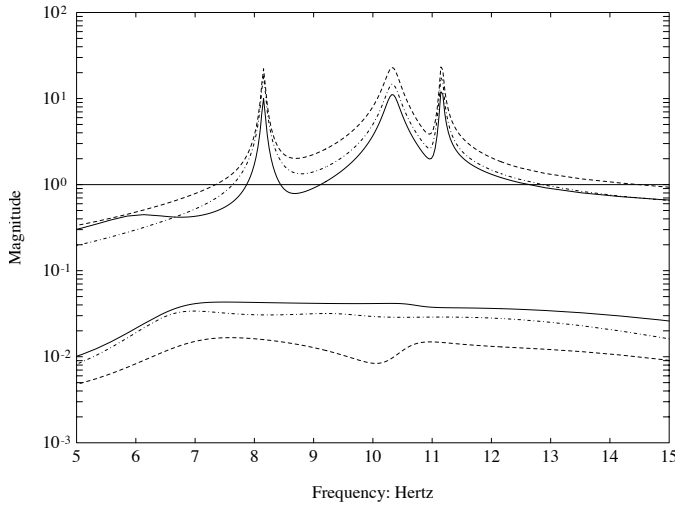


Fig. 12. Maximum and minimum singular values of the loop gains for  $K_1$  (solid),  $K_2$  (dashed) and  $K_3$  (dot-dash)

gest that the level of uncertainty associated with these modes must be well characterized in order to do this in a robust manner.

Controllers  $K_2$  and  $K_3$  roll off significantly faster beyond 30 Hz, gain stabilizing the modes greater than 30 Hz.  $K_3$  exhibited a small amount of local limit cycle behavior. This could possibly come from the 32 Hz mode which is not gain stabilized.  $K_2$ , the least well performing controller, rolls off quickly and exhibited no stability problems.

Singular value analysis is also useful for examining the performance in the lower frequency modes. Figure 12 shows both the maximum and minimum singular values of the loop gain in this frequency range.

The minimum singular value of the loop gain appears to give a good indication of the relative performance of the different controllers. Theoretically, this is only a lower bound on the performance and may be misleading in multiple-input, multiple-output systems. The higher values for  $K_1$  and  $K_3$  suggest better performance and this is indeed the case.

Although it is difficult to pick appropriate weights *a priori*, one can use this experimental information to go through another design iteration. It is expected that reducing the perturbation associated with the first mode of the  $K_3$  design would improve performance. Slightly increasing the additive perturbation weight in the region of 30 Hz would be likely to improve the high frequency stability properties of the design.

## VI. CONCLUSIONS

The robust,  $H_\infty/\mu$ -synthesis approach has been used to design a series of vibration suppression controllers in a very lightly damped, multiple-input, multiple-output, flexible structure. The resulting designs significantly increased the damping in the lower frequency modes to the point where in certain directions no modes were discernible.

Several means of modeling the perturbations were studied. There is currently no theoretically based approach for determining the best perturbation bound or how the perturbations

should enter the model structure. Experimentally based iterative procedures are found to be a suitable ad-hoc approach. In this case a design, with a specified perturbation structure and bound, was experimentally tested and the resulting information was used to refine the perturbation model.

A novel eigenvalue perturbation model was applied to this problem and resulted in a controller with good performance. The ability of this approach to independently assign differing levels of uncertainty to each mode is a potential benefit that was not examined in this case.

The more classical means of estimating worst case performance and stability (singular value loop gain analysis) were found to correlate well with the experimental results. There is no theoretical reason to expect this, particularly since the singular values range over a factor of approximately 1000 in certain frequency ranges, and over a factor of about 100 everywhere else.

Some observations on the overall context of this work are in order. The above has shown that it is possible to design controllers which roll-off through the system modes. Experimental evidence suggests that this is particularly sensitive to relatively small changes in the system. The controller which did not achieve gain stabilization of the higher modes was successful for only a short time. Presumably, the system differed more from its identified model as time progressed and the perturbation model used in the design was unable to account for the system changes.

The  $H_\infty/\mu$ -synthesis procedure is an optimization and if the perturbation model does not cover the system uncertainty then a high performance controller can result in instability. This indicates that designing such controllers places significant requirements on the identification and uncertainty characterization procedure in the cross-over frequency region. Practical applications of such controllers may require regularly repeated identification experiments to maintain a well characterized model in this frequency range.

In a complete spaceborne system design, one will also have the option of placing a limited number of passive dampers in the system. The experience here suggests that those dampers should be placed in order to increase the damping in the cross-over frequency range. As the above experiments show, very lightly damped low frequency modes do not pose a problem in this robust design. Similarly, high frequency gain stabilized modes are also not a problem for the controller design. Note that the controller has no effect on these modes — additional damping may be required to meet system objectives that a low bandwidth controller cannot meet. It is hoped that applying damping to the modes in the cross-over region will reduce their sensitivity to small system changes, thereby making both the identification and design problems easier. Experimental verification and quantification of this issue has yet to be resolved.

## ACKNOWLEDGEMENTS

The authors wish to thank Dr. Dankai Liu for his assistance in conducting the experiments. The research described in this paper was carried out by the Jet Propulsion Laboratory,

California Institute of Technology, under a contract with the National Aeronautics and Space Administration.

## REFERENCES

- [1] R. Laskin and M. San Martin, "Control/structure system design of a spaceborne optical interferometer," in *Proc. AAS/AIAA Astrodynamics Specialist Conf.*, Stowe VT, 1989.
- [2] J. Fanson, G. Blackwood, and C.-C. Chu, "Active-member control of precision structures," in *Proc. AIAA 30th SDM Conf.*, pp. 1154–1163, 1989.
- [3] J. Fanson, C.-C. Chu, B. Lurie, and R. Smith, "Damping and structural control of the JPL phase 0 testbed structure," *J. Intell. Material Sys. & Struct.*, vol. 2, pp. 281–300, July 1991.
- [4] G. J. Balas and J. C. Doyle, "Robust control of flexible modes in the controller crossover region," in *Proc. Amer. Control Conf.*, 1989.
- [5] C.-C. Chu, R. Smith, and J. Fanson, "Robust control of an active precision truss structure," in *Proc. Amer. Control Conf.*, vol. 3, pp. 2490–2495, 1990.
- [6] J. Fanson, C.-C. Chu, R. Smith, and E. Anderson, "Active member control of a precision structure with an  $H_\infty$  performance objective," in *Proc. AIAA 31st SDM Conf.*, pp. 322–333, 1990.
- [7] R. Smith, "Procedures for the identification of the precision truss," Tech. Rep. JPL D-7791, Jet Propulsion Laboratory, 1990.
- [8] The MathWorks, Inc., Natick, MA,  *$\mu$ -Analysis and Synthesis Toolbox ( $\mu$ -Tools)*, 1991.
- [9] E. Anderson, D. Moore, J. Fanson, and M. Ealey, "Development of an active member using piezoelectric and electrostrictive actuators for control of precision structures," in *Proc. AIAA 31st SDM Conf.*, 1990.
- [10] H. Briggs, "JPL control/structure interaction test bed real-time control computer architecture," in *Proc. 3rd annual Conf., Aerospace Computational Control.*, pp. 739–755, 1989.
- [11] J. Fanson, H. Briggs, C.-C. Chu, B. Lurie, R. Smith, D. Eldred, and D. Liu, "JPL CSI Phase-0 experiment results and real time control computer," 4th NASA/DoD CSI Tech' Conf., Nov. 1990.
- [12] A. K. Packard, *What's new with  $\mu$* . PhD thesis, University of California, Berkeley, 1988.
- [13] J. C. Doyle, J. E. Wall, and G. Stein, "Performance and robustness analysis for structured uncertainty," in *Proc. IEEE Control Decision Conf.*, pp. 629–636, 1982.
- [14] J. Doyle, "Analysis of feedback systems with structured uncertainties," *IEEE Proceedings, Part D*, vol. 133, pp. 45–56, Mar. 1982.
- [15] J. Doyle, K. Glover, P. Khargonekar, and B. Francis, "State-space solutions to standard  $H_2$  and  $H_\infty$  control problems," *IEEE Trans. Auto. Control*, vol. AC-34, pp. 831–847, 1989.
- [16] D. F. Enns, *Model Reduction for Control System Design*. PhD thesis, Stanford University, 1984.
- [17] K. Glover, "All optimal Hankel-norm approximations of linear multi-variable systems and their  $L^\infty$ -error bounds," *Int. J. of Control*, vol. 39, no. 6, pp. 1115–1193, 1984.
- [18] R. Smith, "Eigenvalue perturbation models for uncertain structures: A simulation study," Tech. Rep. JPL D-9809, Jet Propulsion Laboratory, May 1992.
- [19] R. S. Smith, "Modeling real parameter variations in flexible structures with complex valued perturbations," in *Proc. IEEE Control Decision Conf.*, pp. 1638–1639, 1991.



**Roy Smith** (S'79–M'89) received the B.E. (Hons.) and M.E. degrees from the University of Canterbury, New Zealand, in 1980 and 1981 and the M.S.E.E. and Ph.D. degrees from the California Institute of Technology in 1986 and 1990. He has worked in industry and government laboratories on control and instrumentation problems in the areas of: boiler systems; linear accelerators and mass spectrometers; automotive emissions and fuel systems; and flexible structures.

In 1989 he held a position as lecturer at Caltech and in 1990 he joined the University of California, Santa Barbara as an assistant professor in the Electrical and Computer Engineering Department. Roy Smith is a member of IEEE, SIAM, AIAA, and NZAC. His research interests include robust control, identification with uncertain models, and control applications in automotive systems, process control and flexible structures.



**Cheng-Chih Chu** (S'84–M'85) was born in Taiwan in 1955. He received the B.S. degree in control engineering from National Chiao-Tung University, Hsinchu, Taiwan, in 1977 and the M.S. degree in electrical engineering and the Ph.D. degree in control science from the University of Minnesota, Minneapolis, MN, in 1981 and 1985, respectively.

He was with Scientific Systems, Inc. as a Research Engineer from 1985 to 1987. Since 1987, he has been a member of technical staff at Jet Propulsion Laboratory, California Institute of Technology, Pasadena, CA. His research interests include robust control, system identification, and applications to flexible structure control problems. His current research focuses primarily on the development of robust attitude estimation algorithms and autonomous spacecraft pointing and navigation systems. Dr. Chu is a member of IEEE and AIAA.



**Dr. James Fanson** received his B.S. from the University of Wisconsin in 1981, and his M.S. and Ph.D. in 1982 and 1987 from the California Institute of Technology. His interests include active materials and adaptive optics, and control system design. Recently he developed a set of active mirrors used in the correction of the Hubble Space Telescope optical aberration.